

Molecular nanopolaritons: Cross manipulation of near-field plasmons and molecules. I. Theory and application to junction control

Daniel Neuhauser^{a)} and Kenneth Lopata
*Department of Chemistry and Biochemistry, University of California,
 Los Angeles, California 90095-1569, USA*

(Received 4 June 2007; accepted 5 September 2007; published online 18 October 2007)

Near-field interactions between plasmons and molecules are treated in a simple unified approach. The density matrix of a molecule is treated with linear-response random phase approximation and the plasmons are treated classically. The equations of motion for the combined system are linear, governed by a simple Liouvillian operator for the polariton (plasmon+molecule excitation) dynamics. The dynamics can be followed in time or directly in frequency space where a trace formula for the transmission is presented. A model system is studied, metal dots in a forklike arrangement, coupled to a two level system with a large transition-dipole moment. A Fano-type resonance [Phys. Rev. **103**, 1202 (1956)] develops when the molecular response is narrower than the width of the absorption spectrum for the plasmons. We show that the direction of the dipole of the molecule determines the direction the polariton chooses. Further, the precise position of the molecule has a significant effect on the transfer. © 2007 American Institute of Physics.
 [DOI: [10.1063/1.2790436](https://doi.org/10.1063/1.2790436)]

I. INTRODUCTION

Plasmonics is an emerging field which examines the transfer of light through surface plasmons, i.e., collective excitations.^{1,2} Advances in fabrication and handling of sub-wavelength structures, such as metal dots with sizes of tens of nanometers and even smaller, have led to subwavelength studies of plasmon motion and transfer. For example, plasmon arrays were excited on one side with emerging light on the other,^{2,3} and collection of plasmons with different frequencies was excited and then followed once the driving pulse is turned off, to see their decoherence in time.⁴ Plasmons are generally described well by classical dynamics down to as little as subnanometer distances where electron transfer can occur. Plasmons' wavelength can be tuned by using different materials and different geometries,⁵ core shell geometries, in particular, are widely tunable, with extremes from the UV to the IR.^{6,7} As plasmons can be localized, this raises an interesting ability to drive electromagnetic energy into well-controlled and confined regions.^{2,8} Plasmons are essentially dipole and higher moments of surface charge, and as such have short-range (R^{-3} or faster decaying) interactions, and therefore have been very useful in nanometric applications, using the shift of the absorption of a dipole-coupled pair of nanodots.⁹ Further, because of their collective nature and the large number of excitations, electromagnetic energy will typically be transferred in the near field through plasmons, which can be manipulated and multiplexed.¹⁰

Another interesting feature is polarization. Near-field radiation supports three polarizations, as, in addition to transverse excitations, it also supports longitudinal motion. The frequencies of each polarization undergo curve crossing

which leads to facile transfer between polarizations, and this is predicted to lead to sharp reflections and negative refraction.¹¹

The consistent treatment of the propagation of plasmons on the subwavelength scale has attracted much attention.^{3,12-16} For example, there has been several works on coupling of molecular dots¹⁷ using electrodynamic methods in both time and frequency domains^{18,19} as well as explicit plasmon hybridization approaches^{14,15,20} and time-dependent density functional theory (DFT) approaches;^{7,12} further, simplified studies of propagation along chains of molecules^{11,21} have yielded dispersion curves with conical intersections which lead to negative refraction and facile transport between the components.¹¹

When plasmons interact with matter, a combined excitation emerges: a polariton. Polaritons have fascinating properties; for example, in the solid state, Bose-Einstein condensates of relatively high temperature polaritons (19 K and higher) have recently emerged;²² polaritons have also found increasing applications in terahertz radiation studies.²³ For near-field applications (see, e.g., Ref. 24) the relevant question is the interaction of the light from the tip with molecules. This is exactly the problem that occurs when light emerges from a tip to interact with a molecule, as in, e.g., near-field scanning optical microscopy^{16,25} and surface-enhanced Raman spectroscopy, where the enhanced fields near a surface are used to magnify the excitation of a molecule.²⁶ A closely related problem is ac conductivity, where light transfers through molecules, typically by dipole coupling.^{7,27} Note that here our focus is not only on the molecular response but also on the transmission of the polariton.

Plasmons and molecules have different scales, nanometers and tens of nanometers for the plasmons and subnanometers for molecules. The difference in scales needs to be

^{a)}Electronic mail: lopata@chem.ucla.edu

bridged. Further, the polariton is a combined structure, so its treatment necessitates consideration of both matter and radiation.

In this work we present a simple yet quantitative approach for the interaction of plasmons and molecules. Essentially, our approach is a combination of a basis expansion for the plasmon modes, with a linear-response assumption for the molecule. The close-coupling expansion is very efficient in handling large scale structures. The linear-response assumption is the same as linear-response time-dependent Hartree-Fock or DFT, leading to random phase approximation (RPA), an approach which is very accurate for molecules. The combined resulting approach is similar to the independent boson model (for chemistry uses see, e.g., Ref. 28). The combination leads to a polariton basis set and a Liouville-type evolution operator, with correlation functions, as derived here, that are akin to well-known transmission-type trace formulae. The Liouville-type operator is very efficient to propagate and invert, as it is not explicitly frequency dependent, even though it yields a frequency-dependent Drude refraction index.

The model is developed in Sec. II; Sec. III presents results, and conclusion then follow in Sec. IV. Appendix A briefly presents RPA, and the polariton model is extended to finite difference time domain (FDTD) treatment of the radiation part in Appendix B.

II. EQUATIONS OF MOTION

A. Plasmon equations of motion

Plasmons are charge waves that propagate on surfaces. Here our derivation for the plasmons follows (with generalized notation) Ref. 15.

In the classical approximation where the plasmons are purely surface waves and have zero penetration depth, one starts with a Lagrangian describing the kinetic energy of the plasmons and their potential energy. Assuming longitudinal motion, the electron velocity in each material is written as a gradient of a velocity-potential,

$$\mathbf{u} = \nabla \eta, \quad (1)$$

and the electron current is, therefore,

$$\mathbf{j} = n_0 e \mathbf{u} = n_0 e \nabla \eta, \quad (2)$$

where we introduced the electron density in the material and the (negative) charge of the electron.

Away from the boundaries of the light-conducting structures, i.e., within any dot or fiber, the density of the electrons will equal that of the background and will be constant in time; therefore, the continuity equation,

$$0 = \dot{n} + \nabla \cdot \mathbf{j} = \dot{n} + n_0 e \nabla^2 \eta, \quad (3)$$

becomes then (away from the boundaries)

$$\nabla^2 \eta = 0. \quad (4)$$

This Poisson-type equation is then solved for the velocity potential; the results are then presented as a basis-set expansion as

$$\eta = \sum_J \dot{C}_J(t) f_J(\mathbf{r}), \quad (5)$$

where the basis function satisfy within the boundaries of the devices $\nabla^2 f_J = 0$, and the time-dependent coefficients are written as derivatives with respect to time for convenience in the derivation. The expansion parameter J runs over all the basis function. (For example, for a sphere the basis functions will be spherical harmonics times a power law, etc.)

The assumption that the charge densities are nonvanishing only on the surface is equivalent to writing the electron densities as

$$n(\mathbf{r}, t) = n_0(\mathbf{r}) + \sigma(\mathbf{r}, t) |\nabla \chi| \delta(\chi(\mathbf{r})), \quad (6)$$

where the background density $n_0(\mathbf{r})$ equals n_0 inside the plasmon carrying structures and vanishes outside; $\chi(\mathbf{r})$ is a function which characterizes the surfaces, i.e., is vanishing on the surface of each structure and its gradient, and we define $\mathbf{n}(\mathbf{r}) = \nabla \chi / |\chi|$ the normalized gradient to the surface [note the different meanings of $\mathbf{n}(\mathbf{r})$, $n(\mathbf{r})$]. The continuity equation on the surface then becomes (after integrating perpendicular to the surface, to remove the delta function)

$$\dot{\sigma} = n_0 e \mathbf{n}(\mathbf{r}) \cdot \nabla \eta, \quad (7)$$

so that

$$\sigma = \sum_J C_J(t) s_J(\mathbf{r}), \quad (8)$$

where

$$s_J(\mathbf{r}) = n_0 e \mathbf{n}(\mathbf{r}) \cdot f_J(\mathbf{r}). \quad (9)$$

Therefore, the basic time-dependent variables characterizing the plasmons are the expansion coefficients $C_J(t)$.

The next step is the derivation of the equations for the plasmons. There are two alternating methods. An elegant approach uses the Lagrangian for the plasmons. An alternate, simple approach is to use the Drude formula. This has an added advantage in that the Drude damping (friction) term is easily incorporated in the formalism, so that the absorption linewidth is included. We briefly review both derivations.

The plasmons' kinetic energy can be written in terms of the electron's velocity and mass

$$\begin{aligned} T_p &= \frac{m n_0}{2} \int u^2(\mathbf{r}) d\mathbf{r} \\ &= \frac{m n_0}{2} \int \nabla \eta \nabla \eta d\mathbf{r} \\ &= \frac{m n_0}{2} \int \eta \nabla \eta dS - \frac{m n_0}{2} \int \eta \nabla^2 \eta d\mathbf{r} \\ &= \frac{m}{2e} \int \eta \dot{\sigma} dS, \end{aligned} \quad (10)$$

where the last equality presents the kinetic energy in terms of a surface integral over the device (where the surface element is $d\mathbf{S} = \mathbf{n} dS$). This expression is readily converted to a bilinear expression in terms of the plasmon coefficients, with the final result that the total kinetic energy is

$$T_p = \frac{1}{2} \sum_{J,K} \dot{C}_J \dot{C}_K M_{JK}, \quad (11)$$

where we introduced the symmetric mass matrix

$$M_{JK} = \frac{m}{e} \int s_J s_K dS. \quad (12)$$

The potential energy is similarly

$$V_p = \frac{1}{2} \int \frac{\sigma(\mathbf{r}, t) \sigma(\mathbf{r}', t')}{|\mathbf{r} - \mathbf{r}'|} dS dS', \quad (13)$$

where the integral is over all surfaces. This integral also has a bilinear form

$$V_p = \frac{1}{2} \sum_{JK} V_{JK} C_J C_K, \quad (14)$$

where the coefficients are

$$V_{JK} = \int \frac{s_J(\mathbf{r}) s_K(\mathbf{r}')}{|\mathbf{r} - \mathbf{r}'|} dS dS'. \quad (15)$$

There is an additional contribution to the potential energy from the molecule, V^M , which is discussed later in the paper.

The plasmon's Lagrangian is then

$$L_p = T_p - V_p = \frac{1}{2} \sum_{J,K} \dot{C}_J M_{JK} \dot{C}_J - \frac{1}{2} \sum_{JK} V_{JK} C_J C_K, \quad (16)$$

leading to the equation of state for the plasmons,

$$\sum_K M_{JK} \ddot{C}_J = - \sum_K V_{JK} C_K. \quad (17)$$

The alternate derivation starts from Drude's model for the forces on the electron,

$$\dot{\mathbf{u}} = - \frac{e \nabla \Phi}{m} - \frac{\mathbf{u}}{\tau}, \quad (18)$$

where we introduced the decay time of the excitations in the material, and the electrostatic potential,

$$\Phi(\mathbf{r}) = \int \frac{s_J(\mathbf{r}')}{|\mathbf{r} - \mathbf{r}'|} dS'.$$

Plugging in the definition of the velocity in terms of the velocity potential leads to

$$\dot{\eta} = - \frac{e\Phi}{m} - \frac{\eta}{\tau}, \quad (19)$$

which, after a straightforward derivation, leads to the final equation for the plasmons,

$$\sum_K M_{JK} \left(\ddot{C}_K + \frac{\dot{C}_K}{\tau_K} \right) = - \sum_K V_{JK} C_K, \quad (20)$$

which has the same form as before, except for an additional Drude damping term. Note that the derivation assumed that τ is constant, at least within a given structure, although in reality τ can be dependent on the material, so in the final formula we labeled it as dependent on the plasmon; τ is analogous to an absorbing potential but will be a physical

parameter responsible for the attenuation dispersion; the analogy is developed further below.

The derivation above neglected the role of the dielectric constant surrounding the medium and the background asymptotic dielectric in the metals; these effects can be introduced by modifying the matrix elements M_{JK} and V_{JK} , and more fundamentally, can be introduced by the FDTD model (see Appendix B).

B. Molecular part

The molecular part will be treated using linear response, i.e., a RPA. The total density matrix for the molecule is written as

$$\rho_{\text{total}} = \rho_0 + \rho, \quad (21)$$

where we introduced the zeroth-order static density matrix (which in the absence of magnetic fields is assumed to be real) and the correction ρ , which is treated to first order in the plasmon fields. The one-body Hamiltonian governing the density matrix is

$$H = h + U(\rho_{\text{total}}) + q, \quad (22)$$

where h is the one-body kinetic and nuclear attraction part; $U(\rho_{\text{total}})$ is the two-body potential, including both the direct electron-electron repulsion on the molecule as well as the exchange-correlation component; and q is the potential on the molecule due to the plasmon,

$$q(\mathbf{r}, t) = \int \frac{\sigma(\mathbf{r}', t)}{|\mathbf{r} - \mathbf{r}'|} dS'. \quad (23)$$

The Heisenberg equation governing the first order density matrix is

$$i \frac{d\rho}{dt} = [H, \rho + \rho_0] - i\gamma\rho = [h, \rho] + [U(\rho + \rho_0) - U(\rho_0), \rho_0] + [q, \rho_0] - i\gamma\rho + O(\rho^2), \quad (24)$$

where we introduced matrix elements for possible additional, phenomenological T_2 damping of the matrix elements [note that $\gamma\rho$ is an element by element multiplication, i.e., $(\gamma\rho)_{ij} = \gamma_{ij}\rho_{ij}$].

The most important term in this context is the driving term due to the plasmon, $[q, \rho_0]$. To obtain it we introduce a basis set used for the expansion of the density matrix and note that the matrix elements of the potential are then defined as

$$q_{ij}(t) = \int \frac{\phi_i(\mathbf{r}) \phi_j(\mathbf{r}) \sigma(\mathbf{r}', t)}{|\mathbf{r} - \mathbf{r}'|} d\mathbf{r} dS'. \quad (25)$$

From the definition of the charge density in terms of the plasmon we get the driving term

$$[q, \rho_0]_{ij}(t) = \sum_J \left(\sum_k q_{ik,J} \rho_{0kj} - \rho_{0ik} q_{kj,J} \right) C_J(t), \quad (26)$$

where

$$q_{ij,J} = \int \frac{\phi_i(\mathbf{r})\phi_j(\mathbf{r})s_J(\mathbf{r}')}{|\mathbf{r} - \mathbf{r}'|} d\mathbf{r}dS'. \quad (27)$$

To get working equations for the density matrix, we define as usual in RPA the real and imaginary parts of the linearized density matrix,

$$\begin{aligned} X_{ij} &= \text{Re}(\rho_{ij}), \\ Y_{ij} &= -\text{Im}(\rho_{ij}). \end{aligned} \quad (28)$$

These equations are most convenient in the basis set of occupied orbitals in, e.g., a Hartree-Fock or Kohn-Sham treatment. Due to the hermiticity of the density matrix and the fact that the only perturbation densities that are nonvanishing couple to the zeroth-order density, it is enough to consider particle-hole excitations, i.e., only store X_{ij}, Y_{ij} , with i and j being an occupied and virtual orbitals. The final equations for X and Y are then obtained by a straightforward derivation (see Appendix A for a brief review), which gives

$$\begin{aligned} \frac{dX_{ij}}{dt} &= \Delta_{ij}Y_{ij} - \gamma_{ij}X_{ij}, \\ \frac{dY_{ij}}{dt} &= -\Delta_{ij}X_{ij} - \sum_{kl} Z_{ijkl}^{2B}X_{kl} - \sum_J q_{ij,J}C_J(t) - Y_{ij}Y_{ij}, \end{aligned} \quad (29)$$

where

$$\Delta_{ij} = \varepsilon_j - \varepsilon_i \quad (30)$$

is the particle hole excitation energy.

C. Molecular and field effects on the plasmon

To conclude we need to include the effects of the molecule on the plasmon as well as external fields. The potential energy associated with the molecule-plasmon interaction is

$$\begin{aligned} V_{\text{total}}^M &= \int \frac{\sigma(\mathbf{r},t)(\rho(\mathbf{r}',t) + \rho_0(\mathbf{r}))}{|\mathbf{r} - \mathbf{r}'|} dSd\mathbf{r}' \\ &= \sum_{ij,J} (\rho_{ij}(t) + \rho_{0,ij})q_{ij,J}C_J(t). \end{aligned} \quad (31)$$

The external field contribution will be

$$\int v_{\text{ext}}(\mathbf{r},t)\sigma(\mathbf{r},t)d\mathbf{S} = \sum_J C_J(t)v_J(t), \quad (32)$$

$$v_J(t) = \int s_J(\mathbf{r})v_{\text{ext}}(\mathbf{r},t).$$

Therefore, the equation of motion for the plasmons becomes

$$\begin{aligned} \sum_K M_{JK}\ddot{C}_K &= -\sum_K V_{JK}C_K - \sum_K M_{JK}\frac{\dot{C}_K}{\tau_K} \\ &\quad - \sum_{ij} (\rho_{ij} + \rho_{ij}^0)q_{ij,J} - v_J(t). \end{aligned} \quad (33)$$

The constant $\sum_{ij}\rho_{ij}^0q_{ij,J}$ can be shown to be very small and serves only to shift the average position of the plasmon by

creating a permanent moment due to the presence of the molecule; it will be therefore ignored below.

D. Combined polariton equations of motion

Equations (29) and (33) yield an equation of motion for the combined polariton. The plasmon momenta are defined as

$$Q_J = \sum_K M_{JK}\dot{C}_K, \quad (34)$$

and a supervector of variables \mathbf{f} of length $2N_J + N_p$ (where N_J is the number of polaritons) is

$$\mathbf{f} = \begin{pmatrix} C \\ Q \\ X \\ Y \end{pmatrix}, \quad (35)$$

i.e., if all virtual and occupied orbitals are used,

$$\begin{aligned} \mathbf{f} &= (C_{J,J=1,\dots,N_J}, Q_{J,J=1,\dots,N_J}, X_{ij,i=1,\dots,N_{\text{occ}},j=1,\dots,N_{\text{vol}}}, \\ &\quad Y_{ij,i=1,\dots,N_{\text{occ}},j=1,\dots,N_{\text{vol}}}). \end{aligned} \quad (36)$$

The evolution equation can then be summarized as

$$\frac{d\mathbf{f}}{dt} = \mathbf{L}\mathbf{f} + \mathbf{v}, \quad (37)$$

where \mathbf{L} is a generalized Liouvillian operator, and from Eqs. (29) and (33), its form will be, with suppressed indices,

$$\mathbf{L} = \begin{pmatrix} 0 & \mathbf{M}^{-1} & 0 & 0 \\ -\mathbf{V} & -\tau^{-1} & -q & 0 \\ 0 & 0 & -\gamma & \Delta \\ -q & 0 & -\Delta - Z^{2B} & -\gamma \end{pmatrix}, \quad (38)$$

while

$$\mathbf{v} = \begin{pmatrix} 0 \\ -v_J \\ 0 \\ 0 \end{pmatrix}. \quad (39)$$

E. Polariton wave functions and transition amplitudes

Once the full Liouville operator for the system is given, it is straightforward to derive wave-function-like expressions as well as transition amplitudes.

In general, the time-dependent solution to Eq. (37) is

$$\mathbf{f}(t) = \int_0^t \exp((t-t')\mathbf{L})\mathbf{v}(t')dt' + \mathbf{f}_0. \quad (40)$$

For a driving field which is a delta pulse in time, and with zero plasmon at earlier times,

$$v_{\text{ext}}(\mathbf{r},t) = v_0(\mathbf{r})\delta(t), \quad (41)$$

it follows that

$$\mathbf{f} = e^{i\mathbf{L}t}\mathbf{v}_0. \quad (42)$$

Typically the driving field will excite one plasmon, or a set of plasmons in one region, which will then propagate in time. Equation (42) can then be used to follow the motion of the combined polariton (plasmon+excitation) in time.

There are many other quantities which can be followed. One will be the field and molecular dynamics if the driving field is periodic, i.e.,

$$v_{\text{ext}}(\mathbf{r}) = \mathbf{v}_0(\mathbf{r})e^{i\omega t}. \quad (43)$$

Then, the solution of Eq. (40) will be (again assuming that at $t=0$ the molecule and plasmons are not excited)

$$\mathbf{f}(t \rightarrow \infty) = e^{i\omega t}D(\omega)\mathbf{v}_0 \quad (44)$$

where frequency-dependent Green's function for the polariton will be

$$D(\omega) = \frac{1}{i\omega - \mathbf{L}}. \quad (45)$$

An alternate goal is to obtain transition probabilities. There are many possible versions of the desired transmissions. To start, presume we excite one or several modes (e.g., excite an initial range of nanodots) with a periodic field; for simplicity we assume that we uniformly excite all nanodots in a given range, denoted by a function θ_I , which is one on excited initial modes and zero otherwise. We can then calculate what will be the summed amplitude collected on another set of modes. The transition probability, defined as the squared amplitude, will be calculated as

$$T(i \rightarrow f) = |\mathbf{a}_F D(\omega)\mathbf{v}_I|^2, \quad (46)$$

where we introduced the initial and final vectors; the initial vector is

$$\mathbf{v}_I = \begin{pmatrix} 0 \\ \theta_I \\ 0 \\ 0 \end{pmatrix}, \quad (47)$$

and the final vector is

$$\mathbf{a}_F = \begin{pmatrix} \theta_F \\ 0 \\ 0 \\ 0 \end{pmatrix}. \quad (48)$$

Equation (46) is automatically recasted as

$$\text{Tr}(W_F D^\dagger(\omega) P_I D(\omega)), \quad (49)$$

where we introduced the projectionlike operators,

$$P_I = \mathbf{v}_I \mathbf{v}_I^\dagger, \quad (50)$$

$$W_F = \mathbf{a}_F \mathbf{a}_F^\dagger.$$

Note that these operators are also valid for coherent illumination of more than one plasmon, where the initial vector is nonzero for several plasmons.

The same generic form of a correlation function involving $D(\omega)$, $D^\dagger(\omega)$ appears for many other possible transition amplitudes. For example, one may ask how much energy is absorbed per unit time from the system on one or more plasmons in the desired final region. Denoting by θ_F a projection to the final region of interest, and presuming the mass tensor does not couple plasmons from different regions, the desired energy is then

$$E_F = \frac{Q\theta_F M^{-1}Q}{2}, \quad (51)$$

so that

$$\frac{dE_F}{dt} = Q\Gamma_F \dot{Q}, \quad (52)$$

where we introduced an absorbing-potential-like (fluxlike) term,

$$\Gamma_F = \frac{1}{2}\theta_F \left(\frac{1}{\tau} M^{-1} + M^{-1} \frac{1}{\tau} \right). \quad (53)$$

Therefore, the proper correlation function will be

$$\text{Tr}(\Gamma_F D^\dagger(\omega) P_I D(\omega)). \quad (54)$$

Similarly, we can write the symmetric correlation function which measures, for a given energy flux due to friction from the first plasmon, how much energy flux goes to the last plasmon; the correlation function will be stipulated, by analogy to the molecular scattering expression,²⁹ to be

$$P_{\Gamma\Gamma}(i \rightarrow F) = \text{Tr}(\Gamma_F D^\dagger(\omega) \Gamma_I D(\omega)). \quad (55)$$

To conclude this section, we note that the formulation presented here is easily extended beyond linear response. For a self-consistent field (SCF)-type ansatz,³⁰ the combined system is described by separate plasmons and a (nonperturbative) density matrix. The nonlinear evolution operator is defined by Eq. (33) and by the Heisenberg equation for the total density matrix,

$$i\dot{\rho}_{\text{total}} = [h_0 + U(\rho_{\text{total}}) + \nu, \rho_{\text{total}}]. \quad (56)$$

This will be studied in later publications, for, e.g., tackling multiharmonic emission from molecules acted on by plasmons from fibers and dots.

III. RESULTS

For the model, we chose a simple system which shows nontrivial effects.

For the plasmons, a set of metal nanodots is considered. For each dot, only the three dipole plasmons are used. The expansion functions for the plasmons are then

$$f_J(\mathbf{r}) = \frac{r}{\sqrt{b_J^3}} Y_{1m_J}(\Omega), \quad (57)$$

$$s_J(\mathbf{r}) = \frac{n_0 e}{\sqrt{b_J^3}} Y_{1m_J}(\Omega),$$

where the distances and solid angles are measured relative to the position of the dot associated with the J th plasmon, b_J is

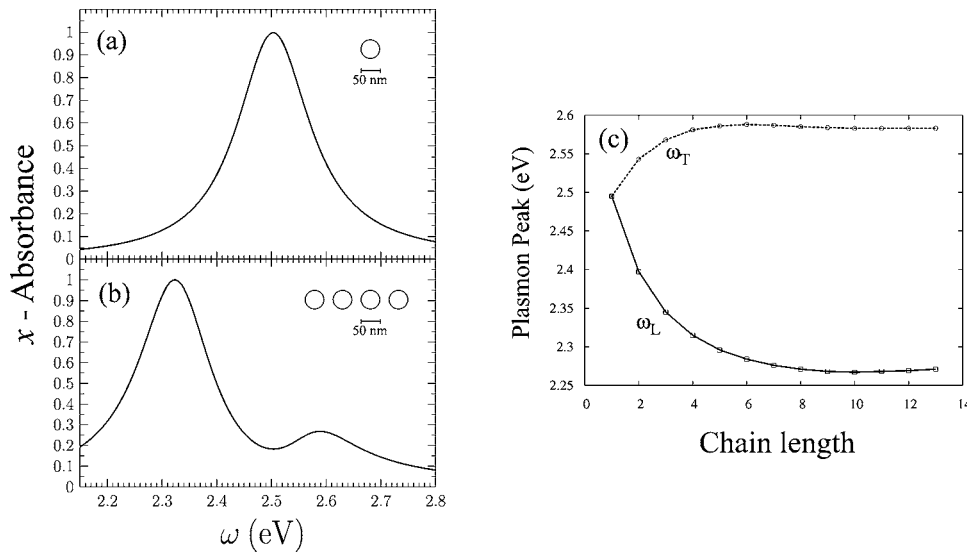


FIG. 1. Normalized absorption spectrum for a single gold nanoparticle (a) and for a linear chain of four particles coherently illuminated with x -polarized light (b). The maximum absorbance frequency as a function of chain length is shown in (c), for both longitudinal (x polarized) excitations and for transverse (y or z polarized) excitations. The resonant frequencies of the chains are found to saturate after approximately four particles. The results are essentially identical to FDTD results (Ref. 31).

its radius, and m denotes the polarization of the plasmon. The plasmon mass vector is then easily shown to be

$$M_{JK} = \delta_{JK} n_0 m_e. \quad (58)$$

The diagonal part of the potential matrix is also simple,

$$V_{JJ} = n_0 m_e \omega_J^2, \quad (59)$$

where formally the surface-dipole plasmon frequency depends only on the density,

$$\omega_J = \sqrt{\frac{4\pi n_0 e^2}{3m_e}}. \quad (60)$$

Materials with different densities, or more complicated geometries such as nanoshells, will produce different plasmon frequencies.

Assuming the dots are sufficiently far apart, the off-diagonal potential matrix elements are essentially that of two coupled dipoles,

$$V_{JK} = n_0^2 e^2 (b_J b_K)^{3/2} \frac{R^2 \delta_{m_J m_K} - 3R_{m_J} R_{m_K}}{R^5}, \quad (61)$$

where R is the distance vector between dots J and K and m_J and m_K ($=1, 2, 3$ for spherically symmetric dots) are the indices for the surface plasmon polarization on dots J and K , respectively.

For all simulations, we took $n_0 = 0.009 \text{ bohr}^{-3}$, similar to the values for Au and Ag. The simplest plasmon model yields a surface dipole plasmon frequency of $\sqrt{4\pi n_0 e^2 / 3m_e} = 5.2 \text{ eV}/\hbar$; to fit to experimental values we have taken a much smaller value, $\omega_s = 2.5 \text{ eV}/\hbar$. The Drude damping time was taken as 6 fs, appropriate for Au.

To study the model, we first examine it relative to known results for a systems of plasmons alone. Figure 1 shows the absorption of radiation of a single 25 nm radius particle and a chain of four such dots with center to center distance of 75 nm, when a totally symmetric pulse is used, i.e., a pulse which excites all plasmons identically and simultaneously. This figure is to be compared with the work of Ref. 31 (and

Ref. 2), employing similar parameters for the dots and using FDTD; very similar results are obtained.

The absorption spectrum when only one dot is present is shifted when a completely symmetric longitudinal pulse is used with four metal dots; the symmetric pulse excites the lowest bound wave of the four-dot system, which is shifted relative to the one-dot pulse, and in addition a second plasmon resonance state is more weakly excited. The reason for the two resonances is physically simple. The lowest resonance is associated with an eigenvector in which the dipoles of the two inner dots are strong in one direction, and the two dipoles on the outer dots have the same sign as the inner dots but are weak; the reason is that the leftmost and rightmost dots only interact with dots on one side, while dots in the middle interact with both sides. Therefore, the lowest resonance is not associated exactly with a uniform excitation, but with an excitation which is stronger at the middle of the four-dot structure. The exciting field itself will be essentially uniform, so it will weakly overlap—in addition to the (not-exactly uniform) lowest excitation—also with the other symmetric excitation, which is associated with strong dipole of one sign in the outer dots, and weak dipole, of opposite sign, in the two inner dots.

In Fig. 1(c), we also plot the maximum absorption frequency as a function of the number of nanodots, for longitudinal and transverse driving waves (i.e., waves with polarization along the x or y axis, where the dots are placed along the x axis); the shift with the number of nanodots matches well Fig. 3(a) in Ref. 31.

Next, we include the effects of the molecules. The molecule is assumed to be a single level oscillator with frequency ω_M , narrow damping [we used three values, $\gamma = \tau_M^{-1} = 0, (24 \text{ fs})^{-1}, (12 \text{ fs})^{-1}$], and transition dipole \mathbf{d} . The zero damping is a severe restriction, but in practice the results will be valid for a system (atom or molecule) with a narrow absorption line and a large transition dipole moment. The oscillator has two states, 0 and 1, and the transition dipole between the states is

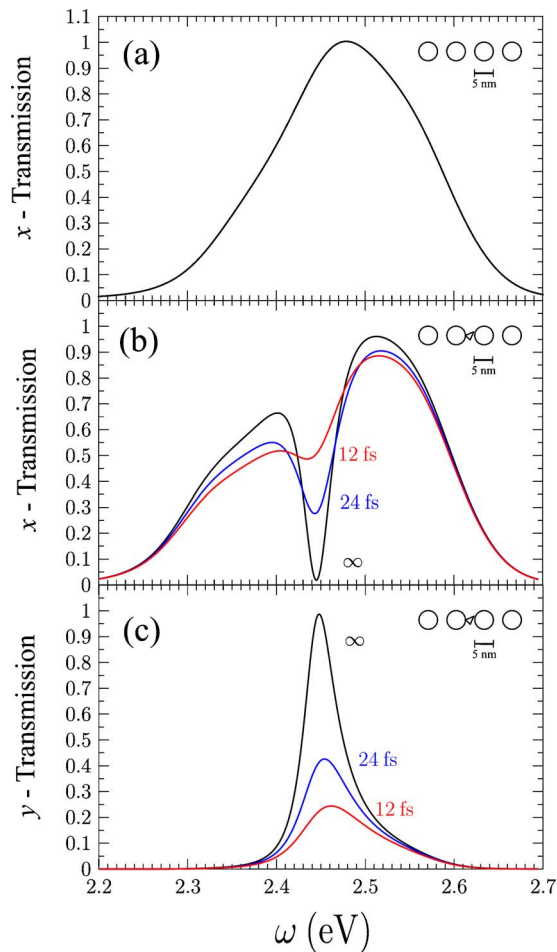


FIG. 2. (Color online) The effect of a dipolar molecule on x -polarized polariton transmission through a linear chain of four gold nanoparticles, the frequency-dependent transmission through the chain without a molecule is featureless (a); while for a chain with a molecule (shown schematically as a triangle) positioned midway between the second and third particles, the transmitted x -polarized intensity shows a very strong resonance dip around the oscillator frequency of the molecule (b). There is also a strong and narrow transmitted y -polarized excitation (c), arising from longitudinal to transverse coupling due to the molecule. Three different molecular dephasing times were used (labeled on plot).

$$\mathbf{d} \equiv \int \phi_0(\mathbf{r})(\mathbf{r} - \mathbf{r}_J)\phi_1(\mathbf{r})d\mathbf{r}. \quad (62)$$

Using a first order expansion, the coupling matrix element becomes

$$q_{01,J} \equiv \int \phi_0(\mathbf{r})\phi_1(\mathbf{r})(\mathbf{r} - \mathbf{r}_J) \nabla \left. \frac{s_J(\mathbf{r}')}{|\mathbf{r} - \mathbf{r}'|} \right|_{\mathbf{r}=\mathbf{r}_J} dS, \quad (63)$$

leading, in the dipole approximation, to

$$q_{01,J} \equiv n_0 e b_J^{3/2} \frac{R^2 d_{m_J} - 3\mathbf{d} \cdot \mathbf{R} R_{m_J}}{R^5}. \quad (64)$$

We note that the formalism is not limited to a dipole approximation; for dots and molecules that are sufficiently close, higher order terms as well as the permanent dipole term have to be considered.

Figure 2 shows the effect of placing a molecule in a chain of four metal dots, oriented along the x axis. Here we

used a much smaller set of dots, with radius of 2.5 nm and center to center separations of 7.5 nm. The molecular transition dipole matrix element is fairly large, ~ 4 a.u., and we used three values of decreasing molecular dephasing time (increased damping; increased absorption linewidth). We assume that the molecular dipole is oriented at a 45° to the plasmon chain and that the molecule is midway between the second and third metal dots. We use Eq. (54) to study the reactivity, by exciting the leftmost molecule with x -polarized light, and measuring the polarized-light intensity at the rightmost molecule. The effect is very strong; a Fano-resonance-like³² dip develops in the transmission factor for driving with an x -polarized light and obtaining an x -polarized light (i.e., a longitudinal to longitudinal transition). An even more striking effect is a strong and very narrow longitudinal \rightarrow transverse excitation, with a width much narrower than that of the plasmon-only spectrum. In essence, the molecule scatters amplitude from one polarization to another, over a narrow frequency range. Increased damping on the molecule strongly reduces the magnitude of this conversion.

Finally, we consider the effect of a molecule on a fork-like junction geometry. This junction is comprised of ten gold nanoparticles of 2.5 nm radius, with center to center separation of 7.5 nm. There is a single “input” chain in the x direction and two “output” chains aligned at 45° with respect to the input, as seen in the insets of Fig. 3. A molecule with a very strong dipole moment (7 a.u.), which is also oriented at 45° with respect to the input chain, is placed 2.5 nm above the x axis (input) of the junction, midway between the third and fourth particles. The oscillator frequency of the molecule was taken to be 2.39 eV/ \hbar . The first particle of the input chain was excited with x -polarized light, and the x -polarized-light intensity was measured on the terminal particles of the top and bottom output chains.

Figure 3 shows the resulting transmission spectra through the top and bottom outputs. The transmission spectrum for the device without the molecule is also shown for comparison. The effect of the xy oriented dipolar molecule is to strongly bias the transmission into the top output of the junction, for a broad range of frequencies around 2.39 eV. This directed transmission phenomenon is severely diminished with increased damping on the molecule. Thus, this fork+molecule device acts as an efficient switch for controlling polariton flow; by varying the strength and orientation of the molecule, as well as its position with respect to the chain, one can choose which of the outputs the polariton travels into. Conversely, this device can be used as a highly sensitive detector of a molecule’s dipole strength, orientation, and position by measuring the relative transmission through to top and bottom outputs.

IV. CONCLUSIONS

In conclusion, we have shown that it is possible to uniformly describe nanoscale polaritons due to near-field interactions with molecules. The description unifies the simple plasmon picture of electromagnetic interactions with linear response for the molecule. The results are completely analo-

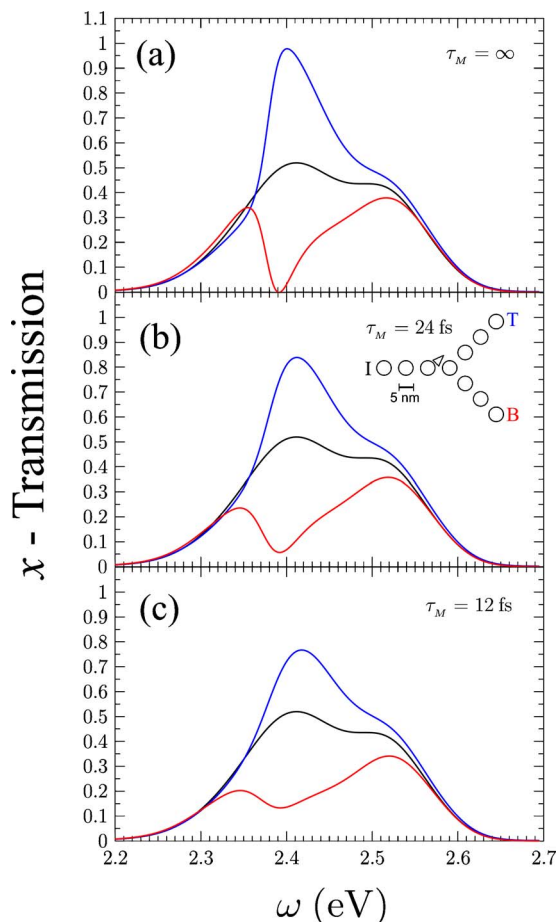


FIG. 3. (Color online) A simple switching junction, which utilizes coupling to a dipolar molecule to guide an x -polarized input polariton (at site “T”) into one of two possible output paths. (a)–(c) differ in the value of the molecule’s dephasing time (values shown on plots). The top (blue) curve shows the x -intensity spectrum for the top output (dot “T”) and the bottom output intensity (dot “B”) is shown below (red). The middle curve shows the transmission for the device with no molecule (both top and bottom outputs then have the same signal). There is a clear bias toward the top output for a wide range of frequencies around the molecule oscillator frequency (2.39 eV); this effect decreases with decreased molecular dephasing time (increased damping). Depending on mode of operation, this device can act as a switch or as molecular sensor. All curves were normalized with respect to the top output.

gous to the well-known state-to-state expressions in molecular dynamics. The use of the RPA simplified the problem by turning it into a set of coupled harmonic oscillators, and the use of a correlation function makes the combined problem analogous to that of molecular scattering or electron transmission, with the combined Liouvillian operator playing the role usually used for a Hamiltonian.

Physically, the interesting phenomenon discussed here is the facile control that can be exerted on the transfer of the plasmons using dipole moments. This raises an intriguing question, whether, if the control is sufficiently significant, the linear-response assumption can break down since the molecule excitation will be beyond linear response. While this will be study in model close-coupling and SCF calculations, the indications of the linear-response study are that molecular motion can significantly affect transfer between

plasmons, as long as the dimensions of the structures carrying the plasmons (or of the end of the tips if a tip configuration is used) are sufficiently small.

There are several directions that emerge from this work and will be extended in future studies. First, we have only studied a simple structure where on each metal dot only the dipole is considered. Future work will consider more complicated structures, which can carry up to a near continuum of states, such as a tip, nanotubes, or skewed structures. Effects of dielectrics will also be incorporated (see also Appendix B).

An additional direction is to consider molecules which have more than one dipole excitation, for example, nanotubes and similar structures, where a set of excitations can be considered; then, of course, the distinction between a molecular dipole and a plasmon is becoming blurred.

Additional effects not considered here but which will be straightforward to incorporate include spins and magnetic fields. More specifically, the spins can be manipulated both through spin orbit effects³³ and through magnetic fields.³⁴

An effect which is straightforward to incorporate is that of nuclear motion. The strongest effects will typically be indirect, i.e., the plasmons will excite molecules, and the molecular electronic excitations will cause nuclear motion. The plasmon will heat or cool the nuclear excitations. Within the RPA, the nuclear motion effects will be that of an additional harmonic oscillator coupling, which will leave the overall Hamiltonian linear; in practice, the Liouville operator will be extended to include the additional nuclear degrees of freedom.

An additional issue is systems where there is physical bonding between molecules and tips. Then, the coupling matrix elements between the molecules and the plasmon need to be calculated more precisely and extend beyond the dipole-dipole order. While numerically involved, the calculations are straightforward.

The effects of chemical bonding on the interactions between the plasmons and the molecule will be more involved, since when there can be electron transfer between the plasmon-supporting structure (e.g., a metal dot) and the molecule. One simple way to account for the coupling will be through using embedding formalisms, in which the total density of the system is divided to an explicitly treated part and a background part, where the latter will support the plasmon here. The two parts can be overlapping, as in several modern embedding approaches; or, alternately, they can be separated. The separation will be done by “carving” a part of the metal dot and treating it explicitly together with the molecule which it supports; the rest of the dot or tip will be treated as a plasmon.

The effect of the polarization of the wave can be quite important, as near-field light supports both longitudinal and transverse excitations, which have different group velocities and interesting conical-intersection effects. These effects were previously studied in an idealized model in which, effectively, the frequency dependence and broadening of the response of the plasmons were ignored.¹¹ A future study will examine polarization effects in the present framework, including the time-dependent response.

The present formulation uses linear response for the dipoles. As mentioned, it is straightforward to go beyond linear response with a SCF formulation where the field induced by the plasmons is propagated at the same time as the molecular density matrix (which will now be far from ρ_0); this can be used to study the modified polaritons in this unique regime of nonlinear response. An intriguing but numerically costly approach is to use influence functionals,³⁵ which in this context will account for the effects of all the modes except the starting mode, leading to a time-dependent kernel for the combined density matrix and higher tensors of the molecule and the driving plasmon mode.

Finally, an intriguing possibility is whether a polariton can undergo lasing. Specifically, since the combined system is essentially a boson, many quanta can be placed. As the intensity becomes higher, the linear-response approximation for the molecule will lose its validity, so more sophisticated formalisms of coupling the boson plasmon bath to a molecule need to be addressed. It is clear, however, that a polariton mode will be able to support multiple bosons as long as the product of the number of bosons times the intensity of the contribution of the density matrix to the mode will be significantly smaller than one; otherwise, the response will be determined as a SCF level.

ACKNOWLEDGMENTS

Discussions with Peter Felker, Igor Ovchinnikov, and Ben Schwartz are gratefully acknowledged.

APPENDIX A: BRIEF OVERVIEW OF THE DERIVATION OF THE RPA

In the ground state, without a plasmon effect, the zeroth-order Kohn-Sham or Hartree-Fock Hamiltonian,

$$h_0 = h + U(\rho_0), \quad (\text{A1})$$

commutes with the zeroth-order density matrix,

$$[h_0, \rho_0] = 0. \quad (\text{A2})$$

Equation (24) can then be rewritten in a superoperator form,

$$i \frac{d\rho}{dt} = Z\rho + [v, \rho_0], \quad (\text{A3})$$

where the meaning of the superoperator is clearest if we include specific indices,

$$i \frac{d\rho_{ij}}{dt} = \sum_{kl} Z_{ij,kl} \rho_{kl} + \sum_J d_{ij,J} C_J(t). \quad (\text{A4})$$

The superoperator in index form can be written as

$$Z_{ij,kl} = h_{ik} \delta_{jl} - h_{ij} \delta_{lk} - Z^{2B}_{ijkl} - i \gamma_{ij} \delta_{ik} \delta_{jl}, \quad (\text{A5})$$

where we introduced the two-body contribution to the density, defined formally as

$$Z^{2B}_{ijkl} = -\frac{1}{\zeta} [U(\rho_0 + \zeta(|k\rangle\langle l| + |l\rangle\langle k|)) - U(\rho_0), \rho_0]_{ij}, \quad (\text{A6})$$

where ζ is a small number inserted to ensure linearity. For a Hartree-Fock description,

$$Z^{2B}_{ijkl} = \sum_n \rho_{0,in} (V_{njkl}^{2B} - V_{jnkl}^{2B}) - \sum_n (V_{inkl}^{2B} - V_{nikl}^{2B}) \rho_{0,nj}, \quad (\text{A7})$$

with different expressions for a density-functional representation. Here we introduced the matrix element of Coulomb electron-electron interaction.

In a diagonal representation,

$$h_0 = \sum_{k=1}^{N_{\text{occ}}+N_{\text{virt}}} |k\rangle \varepsilon_k \langle k|, \quad (\text{A8})$$

$$\rho_0 = \sum_i^{N_{\text{occ}}} |i\rangle \langle i|.$$

Using i and j for occupied and unoccupied levels, the superoperator can be recast. In terms of the real and imaginary terms of the density matrix; Eq. (29) results, with the simplification that now

$$Z^{2B}_{ijkl} = V_{ijkl}^{2B} - V_{jikl}^{2B}, \quad (\text{A9})$$

and, as mentioned, the second term will be modified for a density-functional description, where it accounts for exchange and correlation.

APPENDIX B: POLARITON IN FDTD CALCULATIONS

Although the polariton formalism has been derived here in the framework of plasmon modes, the methodology is equally relevant to other approaches. For example, in modern FDTD approaches, the electric and magnetic fields are supplemented by a single (or multiple) current vector \mathbf{J} that represents the Drude response to the electric field. Upon adding the contribution of the molecule, the relevant equation will read

$$\frac{\partial \mathbf{H}}{\partial t} = -\frac{1}{\mu_0} \nabla \times \mathbf{E},$$

$$\varepsilon_D(\infty) \frac{\partial \mathbf{E}}{\partial t} = \nabla \times \mathbf{H} - \mathbf{J} - \mathbf{J}_M, \quad (\text{B1})$$

$$\frac{\partial \mathbf{J}}{\partial t} = -\Gamma_D \mathbf{J} + \omega_D^2 \varepsilon_0 \mathbf{E},$$

where these equations use the magnetic and electric fields, and the Drude dielectric constant, frequency, damping parameter, and asymptotic refraction index (see, e.g., Ref. 19). The one new ingredient in the equations will be the molecular-induced current, which will read as

$$\mathbf{J}_M(\mathbf{r}) = \sum_{ij} j_{ij} \rho_{ij} \delta(\mathbf{r} - \mathbf{r}_M), \quad (\text{B2})$$

where we introduced the coefficients of current term and the location of the molecule. The only problematic term is the delta function, which involves the position of the molecule. When the electromagnetic fields and \mathbf{J} are represented on grids, the simplest choice for delta function will take the following form:

$$\begin{aligned} \delta(\mathbf{r} - \mathbf{r}_M) &\equiv \frac{1}{d^3\mathbf{r}} \operatorname{sinc}\left(\frac{\pi(\mathbf{r} - \mathbf{r}_M)}{d\mathbf{r}}\right) \\ &\equiv \frac{1}{dxdydz} \operatorname{sinc}\left(\frac{\pi(x - x_M)}{dx}\right) \operatorname{sinc}\left(\frac{\pi(y - y_M)}{dy}\right) \\ &\quad \times \operatorname{sinc}\left(\frac{\pi(z - z_M)}{dz}\right). \end{aligned} \quad (\text{B3})$$

Note that this allows the molecule to be placed in between grid points. This representation is obtained by Fourier transforming the delta function to momentum space analytically (leading to a constant Fourier coefficient) and then transforming it back numerically. Other choices are feasible and may be desirable to reduce the long-range “ringing” of the delta function; for example, one can use the distributed approximating functionals (DAF) composition³⁶ to get a more localized representation of the delta function away from the grid. Alternately, a larger basis set can be used, encompassing both grid points [i.e., sinc-type functions as in Eq. (B3)] as well as a set of localized functions $\chi_l(\mathbf{r})$ describing the plasmon near the molecule, i.e.,

$$\mathbf{E}(\mathbf{r}, t) = \sum_{\mathbf{g}} \mathbf{E}_{\mathbf{g}}(t) \operatorname{sinc}\left(\frac{\pi(\mathbf{r} - \mathbf{r}_{\mathbf{g}})}{d\mathbf{r}}\right) + \sum_l \mathbf{a}_l(t) \chi_l(\mathbf{r}), \quad (\text{B4})$$

where we introduced a summation index over the grid. Note that the set of functions $\chi_l(\mathbf{r})$ will be most efficient when it is made orthogonal to the grid point, so that the set of equations for the grid coefficients and the extra function has a unit overlap matrix. Simulations using this approach will be presented in future work.

Finally, the equations for the electromagnetic field are supplemented by an equation for the molecule, as follows:

$$i \frac{\partial \rho_{ij}}{\partial t} = \sum_{kl} Z_{ij,kl} \rho_{kl} + [\boldsymbol{\mu} \cdot \mathbf{E}(\mathbf{r}_M), \rho_0]_{ij}, \quad (\text{B5})$$

where we introduced the dipole operator on the molecule and have ignored the magnetic coupling to the molecule. Together, Eqs. (B1) and (B5) give a linear set which define the effective evolution operator for this scheme; the usual Heisenberg equation (without the RPA approximation) can be used if nonlinear effects are desired.

¹ S. A. Maier, M. L. Brongersma, P. G. Kik, S. Meltzer, A. A. G. Requicha, and H. A. Atwater, *Adv. Mater.* (Weinheim, Ger.) **13**, 1501 (2001).

² L. A. Sweatlock, S. A. Maier, H. A. Atwater, J. J. Penninkhof, and A. Polman, *Phys. Rev. B* **71**, 235408 (2005).

³ S. A. Maier, P. G. Kik, H. A. Atwater, S. Meltzer, E. Harel, B. E. Koel, and A. A. G. Requicha, *Nat. Mater.* **2**, 229 (2003).

⁴ A. Kubo, K. Onda, H. Petek, Z. J. Sun, Y. S. Jung, and H. K. Kim, *Nano Lett.* **5**, 1123 (2005).

⁵ S. Link and M. A. El-Sayed, *J. Phys. Chem. B* **103**, 4212 (1999).

⁶ E. Prodan, C. Radloff, N. J. Halas, and P. Nordlander, *Science* **302**, 419 (2003); K. Yabana and G. F. Bertsch, *Z. Phys. D: At., Mol. Clusters* **32**, 329 (1995).

⁷ R. Baer, D. Neuhauser, and S. Weiss, *Nano Lett.* **4**, 85 (2004).

⁸ D. J. Sirbully, M. Law, P. Pauzauskie, H. Q. Yan, A. V. Maslov, K. Knutsen, C. Z. Ning, R. J. Saykally, and P. D. Yang, *Proc. Natl. Acad. Sci. U.S.A.* **102**, 7800 (2005).

⁹ C. Sonnichsen, B. M. Reinhard, J. Liphardt, and A. P. Alivisatos, *Nat. Biotechnol.* **23**, 741 (2005); V. M. Shalaev, W. S. Cai, U. K. Chettiar, H. K. Yuan, A. K. Sarychev, V. P. Drachev, and A. V. Kildishev, *Opt. Lett.* **30**, 3356 (2005).

¹⁰ L. Dobrzynski, A. Akjouj, B. Djafari-Rouhani, J. O. Vasseur, M. Bouazaoui, J. P. Vilcot, H. Al Wahsh, P. Zielinski, and J. P. Vigneron, *Phys. Rev. E* **69**, 035601 (2004); V. A. Podolskiy, A. K. Sarychev, E. E. Narimanov, and V. M. Shalaev, *J. Opt. A, Pure Appl. Opt.* **7**, S32 (2005).

¹¹ R. Baer, K. Lopata, and D. Neuhauser, *J. Chem. Phys.* **126**, 014705 (2007).

¹² E. Prodan and P. Nordlander, *Nano Lett.* **3**, 543 (2003).

¹³ E. Prodan, P. Nordlander, and N. J. Halas, *Chem. Phys. Lett.* **368**, 94 (2003); M. Hasegawa and M. Watabe, *J. Phys. Soc. Jpn.* **27**, 1393 (1969); F. Calvayrac, P. G. Reinhard, and E. Suraud, *Phys. Rev. B* **52**, R17056 (1995); B. Montag and P. G. Reinhard, *ibid.* **51**, 14686 (1995); M. Quinten, A. Leitner, J. R. Krenn, and F. R. Aussenegg, *Opt. Lett.* **23**, 1331 (1998); F. I. Baida, D. Van Labeke, Y. Pagani, B. Guizal, and M. Al Naboulsi, *J. Microsc.* **213**, 144 (2004); R. Quidant, C. Girard, J. C. Weeber, and A. Dereux, *Phys. Rev. B* **69**, 085407 (2004); Z. W. Liu, S. Durant, H. Lee, Y. Pikus, N. Fang, Y. Xiong, C. Sun, and X. Zhang, *Nano Lett.* **7**, 403 (2007).

¹⁴ Y. P. Wu and P. Nordlander, *J. Chem. Phys.* **125**, 124708 (2006).

¹⁵ E. Prodan and P. Nordlander, *J. Chem. Phys.* **120**, 5444 (2004).

¹⁶ C. Girard, O. J. F. Martin, and A. Dereux, *Phys. Rev. Lett.* **75**, 3098 (1995).

¹⁷ C. F. Bohren and D. R. Huffman, *Absorption and Scattering of Light by Small Particles* (Wiley, New York, 1983).

¹⁸ A. Taflov and S. Hagness, *Computational Electrodynamics: The Finite-Difference Time-Domain Method*, 2nd ed. (Artech House, Boston, 2000); K. L. Kelly, A. A. Lazarides, and G. C. Schatz, *Comput. Sci. Eng.* **3**, 67 (2001); M. M. Miller and A. A. Lazarides, *J. Phys. Chem. B* **109**, 21556 (2005); C. Girard, *Rep. Prog. Phys.* **68**, 1883 (2005); A. A. Lazarides and G. C. Schatz, *J. Phys. Chem. B* **104**, 460 (2000); G. Gay, O. Alloschery, J. Weiner, H. J. Lezec, C. O'Dwyer, M. Sukharev, and T. Seideman, *Nat. Phys.* **2**, 792 (2006); J. C. Weeber, A. Dereux, C. Girard, G. C. des Francs, J. R. Krenn, and J. P. Gouillon, *Phys. Rev. E* **62**, 7381 (2000).

¹⁹ S. K. Gray and T. Kupka, *Phys. Rev. B* **68**, 045415 (2003).

²⁰ E. Prodan and P. Nordlander, *Chem. Phys. Lett.* **352**, 140 (2002).

²¹ W. H. Weber and G. W. Ford, *Phys. Rev. B* **70**, 125429 (2004).

²² J. Kasprzak, M. Richard, S. Kundermann, A. Baas, P. Jeambrun, J. M. J. Keeling, F. M. Marchetti, M. H. Szymanska, R. Andre, J. L. Staehli, V. Savona, P. B. Littlewood, B. Deveaud, and L. S. Dang, *Nature (London)* **443**, 409 (2006).

²³ N. S. Stoyanov, D. W. Ward, T. Feurer, and K. A. Nelson, *Nat. Mater.* **1**, 95 (2002); K. C. Huang, P. Bienstman, J. D. Joannopoulos, K. A. Nelson, and S. Fan, *Phys. Rev. B* **68**, 075209 (2003).

²⁴ J. R. Krenn and J. C. Weeber, *Philos. Trans. R. Soc. London, Ser. A* **362**, 739 (2004).

²⁵ G. W. Bryant, E. L. Shirley, L. S. Goldner, E. B. McDaniel, J. W. P. Hsu, and R. J. Tonucci, *Phys. Rev. B* **58**, 2131 (1998); P. F. Barbara, D. M. Adams, and D. B. O'Connor, *Annu. Rev. Mater. Sci.* **29**, 433 (1999); J. D. McNeill, D. Y. Kim, Z. H. Yu, D. B. O'Connor, and P. F. Barbara, *J. Phys. Chem. B* **108**, 11368 (2004); A. Lewis, A. Radko, N. Ben Ami, D. Palanker, and K. Lieberman, *Trends Cell Biol.* **9**, 70 (1999); D. A. Higgins, D. A. VandenBout, J. Kerimo, and P. F. Barbara, *J. Phys. Chem.* **100**, 13794 (1996); R. D. Schaller, J. C. Johnson, K. R. Wilson, L. F. Lee, L. H. Haber, and R. J. Saykally, *J. Phys. Chem. B* **106**, 5143 (2002); A. Lewis, U. Benami, N. Kuck, G. Fish, D. Diamant, L. Lubovsky, K. Lieberman, S. Katz, A. Saar, and M. Roth, *Scanning* **17**, 3 (1995).

²⁶ M. Moskovits, *J. Chem. Phys.* **69**, 4159 (1978); H. Metiu, *Prog. Surf. Sci.* **17**, 153 (1984); H. Metiu and P. Das, *Annu. Rev. Phys. Chem.* **35**, 507 (1984); A. Nitzan and L. E. Brus, *J. Chem. Phys.* **75**, 2205 (1981); Z. Kotler and A. Nitzan, *J. Phys. Chem.* **86**, 2011 (1982).

²⁷ M. F. Garcia-Parajo, J. Hernando, G. S. Mosteiro, J. P. Hoogenboom, E. M. H. P. van Dijk, and N. F. van Hulst, *ChemPhysChem* **6**, 819 (2005).

²⁸ K. M. Leung, G. Schon, P. Rudolph, and H. Metiu, *J. Chem. Phys.* **81**, 3307 (1984); R. Baer and R. Kosloff, *ibid.* **106**(21), 8862 (1997).

²⁹ T. Seideman and W. H. Miller, *J. Chem. Phys.* **96**, 4412 (1992).

³⁰ A. K. Gupta and D. Neuhauser, *Int. J. Quantum Chem.* **81**, 260 (2001).

³¹ S. A. Maier, P. G. Kik, and H. A. Atwater, *Appl. Phys. Lett.* **81**, 1714 (2002).

³² U. Fano, *Phys. Rev.* **103**, 1202 (1956).

³³ I. V. Ovchinnikov and D. Neuhauser, *J. Chem. Phys.* **123**, 204714 (2005).

³⁴ O. Hod, E. Rabani, and R. Baer, *J. Phys. Chem.* **108**, 14807 (2004).

³⁵ N. Makri and D. E. Makarov, *J. Chem. Phys.* **102**, 4600 (1995).

³⁶ D. K. Hoffman, G. W. Wei, D. S. Zhang, and D. J. Kouri, *Phys. Rev. E* **57**, 6152 (1998).